Spectral diagnostics and abundances based on a new population of planetary nebulae discovered in the LMC

Warren Reid[1]
Supervisor: Quentin Parker[1,2]

[1]Macquarie University,
Sydney, Australia
[2] Anglo-Australian Observatory

Anglo-Australian Observatory

MACQUARIE UNIVERSITY ~ SYDNEY

SuperCOSMOS scanned UKST Images

R-band, IIIaF

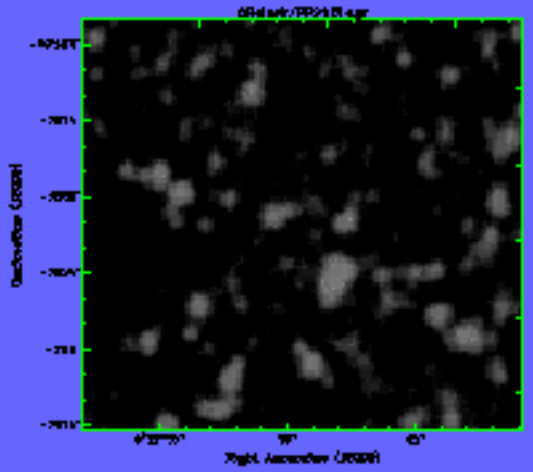

R-band, Tech-pan single exp.

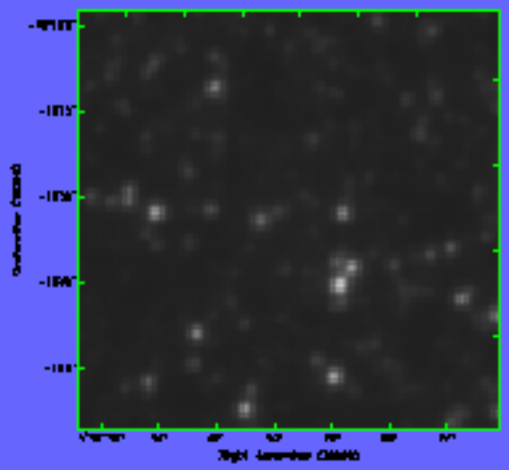

R-band, Tech-pan stacked

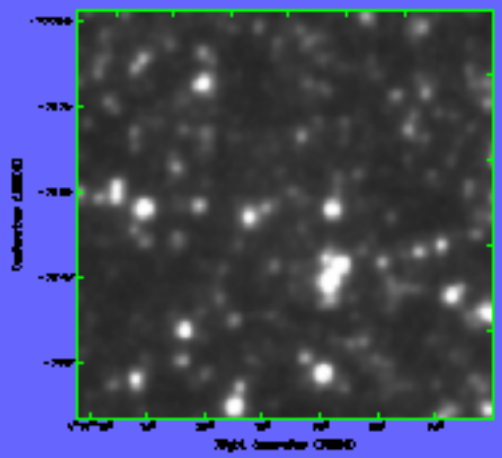

Hα, Tech-pan single exp.

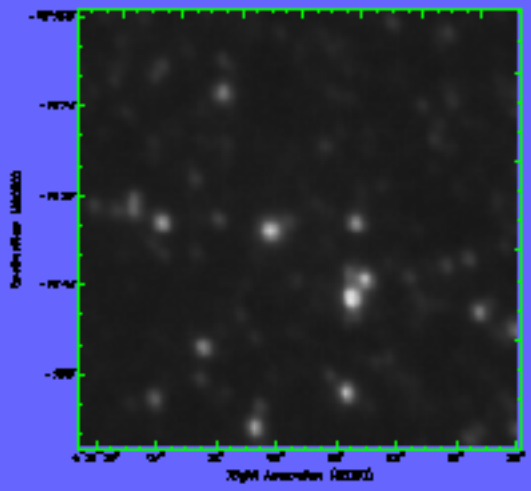

Hα, Tech-pan stacked

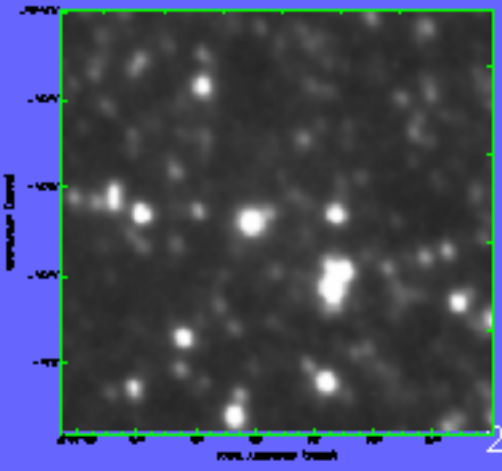

Flux calibration of 2dF spectra

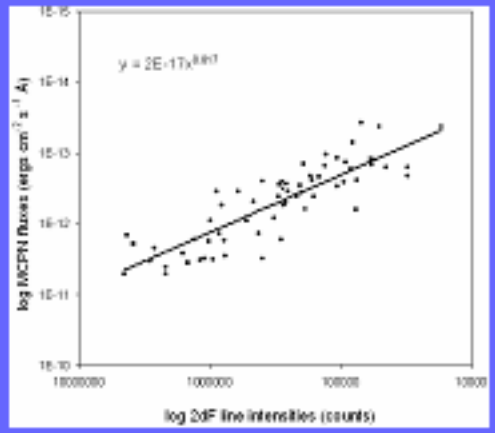

1. Raw fluxes for [OIII]5007 from MCPN are compared with 2dF line intensities for the same objects.

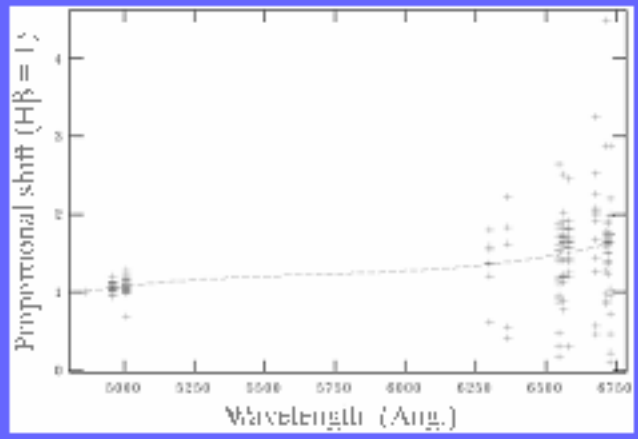

2. With Hβ = 1 for HST fluxes and 2dF line intensities, An increasing shift occurs across the 2dF spectrum.

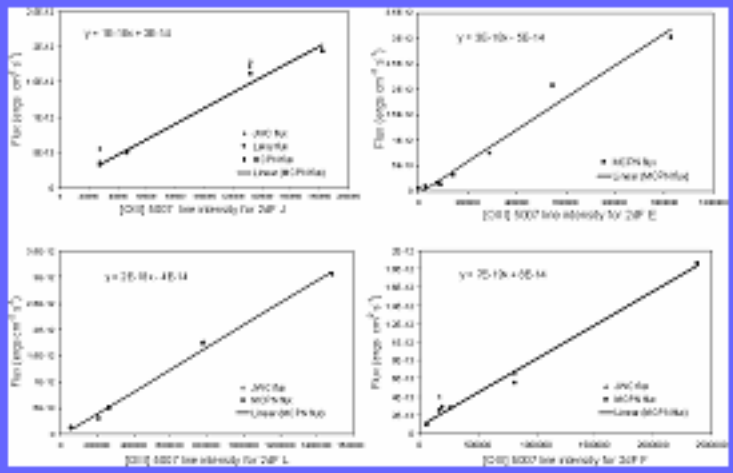

3. Matching of 2dF line intensities to MCPN-based fluxes for individual lines on each field plate produces a calibration equation for each line in each 2dF field.

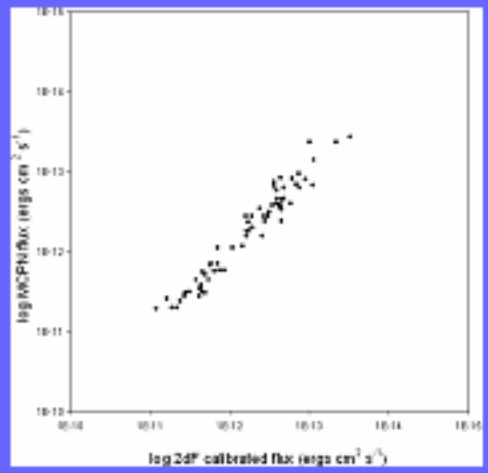

4. The calibrated [OIII]5007Å 2dF line fluxes are Plotted against the published [OIII]5007Å MCPN fluxes.

A Unique Set of Matching Images

- Deep UKST Hα and equivalent R-band images of the entire 25 deg^2 central LMC
- Monolithic, high quality Hα filter
- High-resolution Tech-Pan film
- SuperCOSMOS scanned and co-added exposures. 0.67 arcsec pixels after 15-bit digitized plate scanning. (SHASSA = 48 arcsec resolution WHAM = 3 min)
- Depth reaches R-equivalent ~22 for Hα and R ~21.5 for Red
- IAM data

New PN!

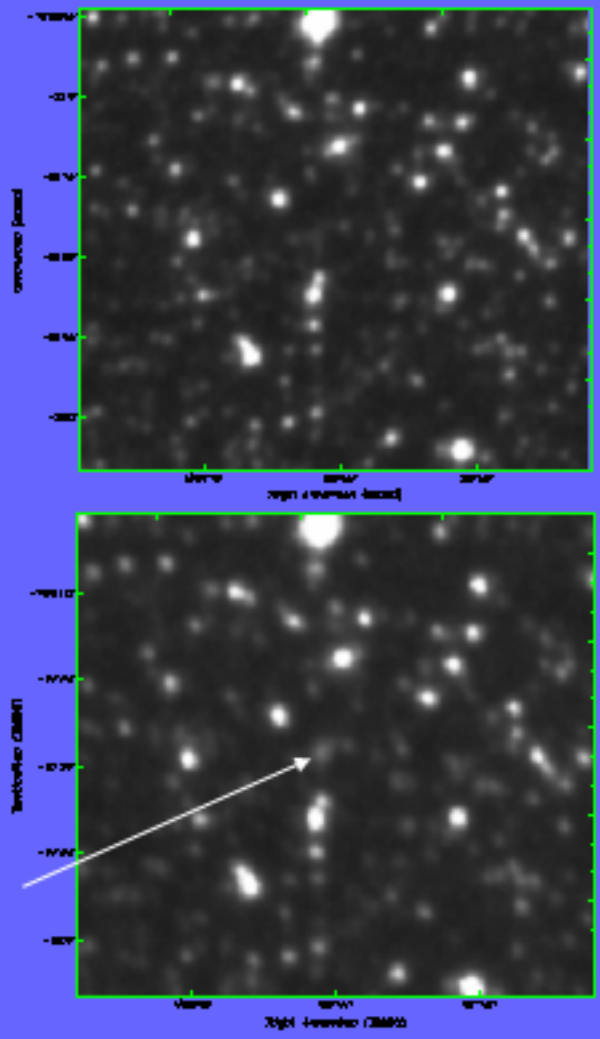

Red
6 x
15min
Stack

Hα
12 x 2hr
Stack

Previously Known PNe Re-identified

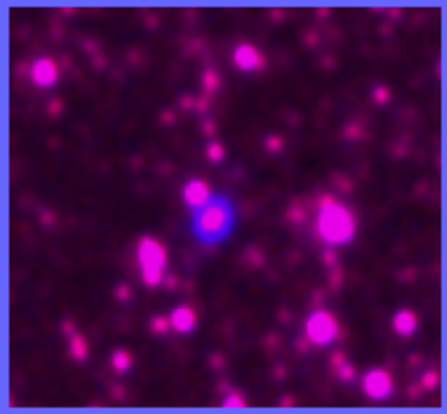

SMP 90

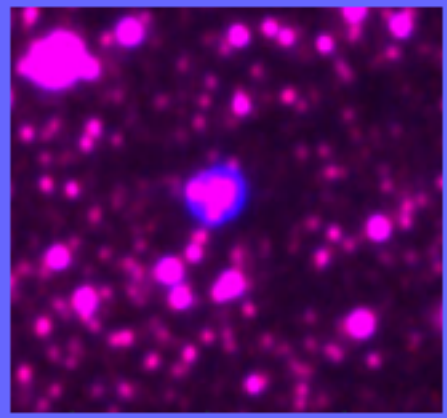

SMP 89

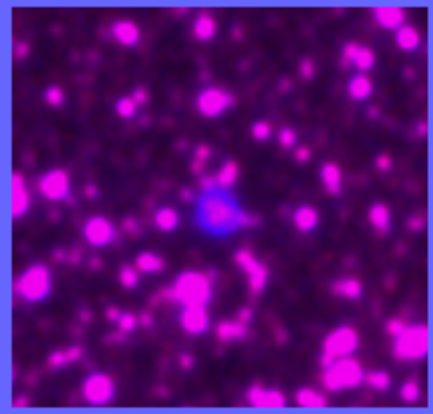

Mo 35

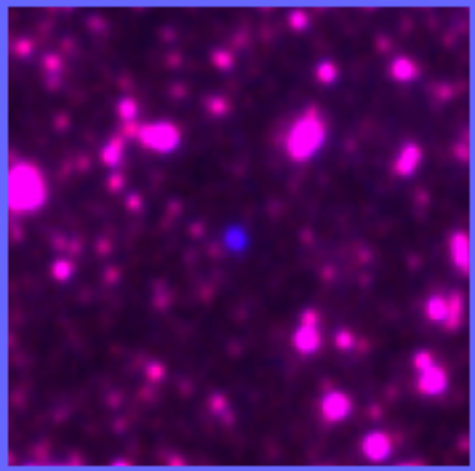

Mo 39

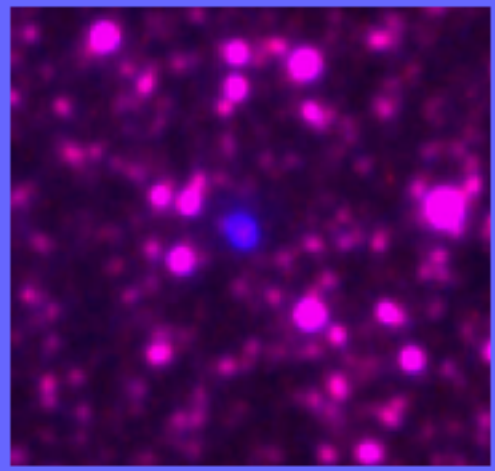

Mo37

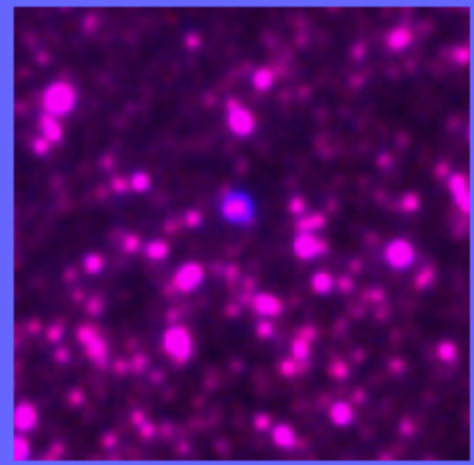

Mo 36

Spectroscopic Follow-up observations

The telescopes used were:	Number of Objects observed
• 2dF on the Anglo Australian Telescope	2,224*
• 1.9m at South African Astronomical Observatory	79
• FLAMES multi-fibre spectrograph on the VLT	1260
• MSSSO 2.3-m telescope	56
• 6dF on the UKST	573

* This includes 3,683 low resolution (300B) and 3,838 high resolution (1200R) spectra

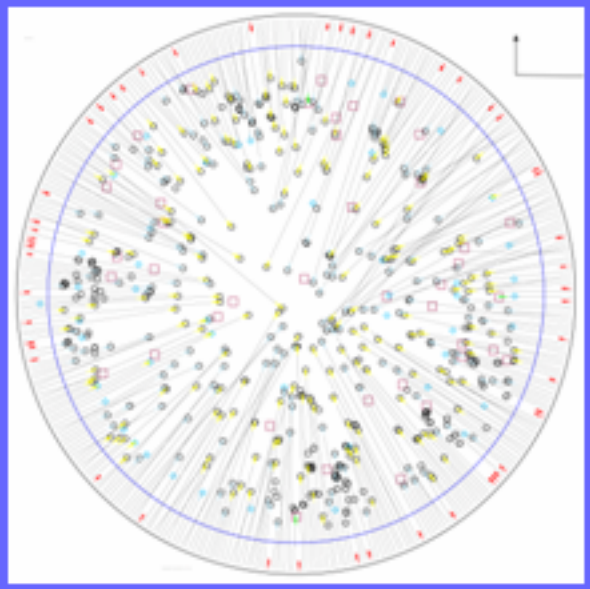

A 2dF field configuration

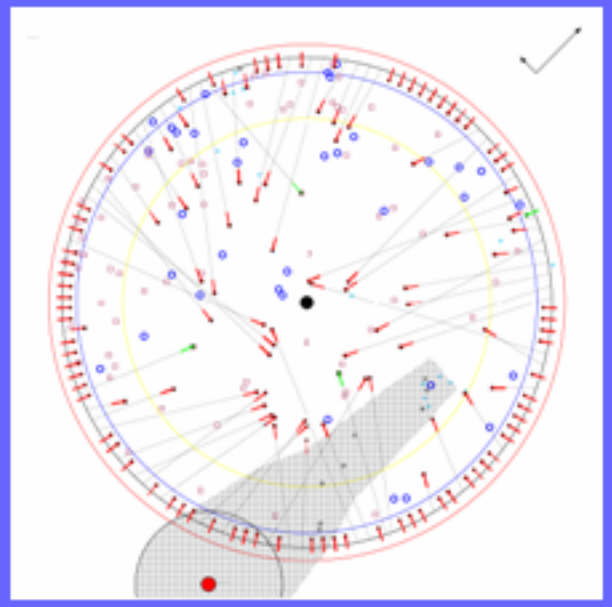

A VLT FLAMES field configuration

Images and Spectra of New PNe

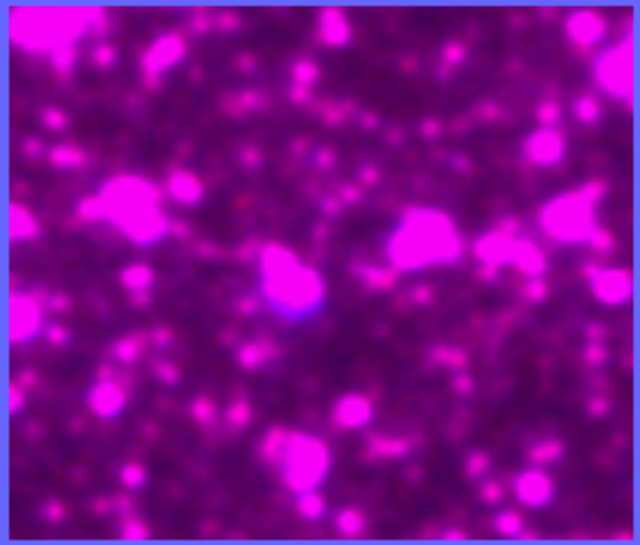

RP 23

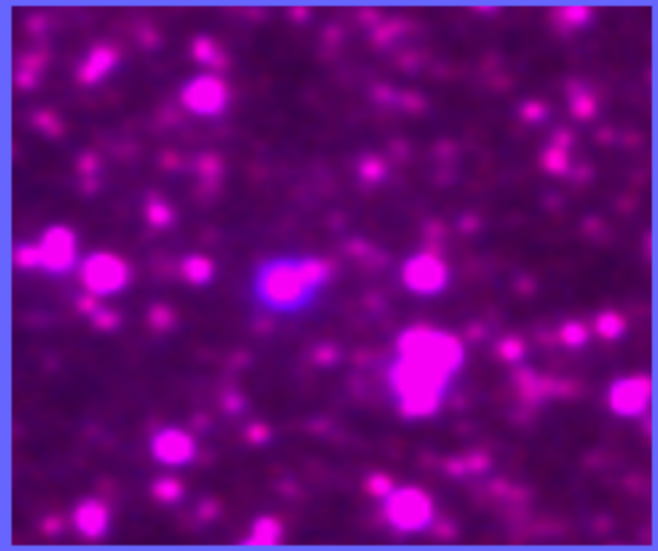

RP 25

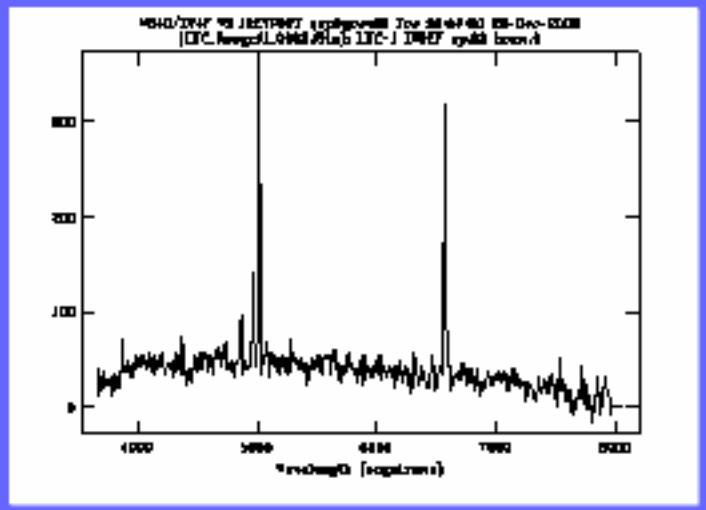

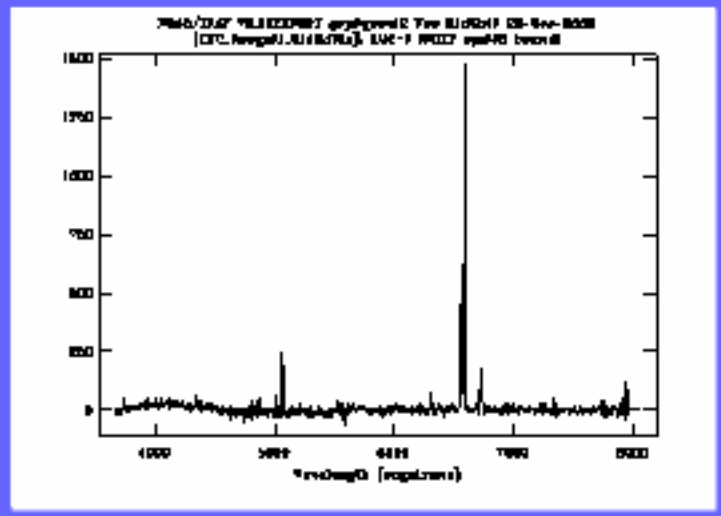

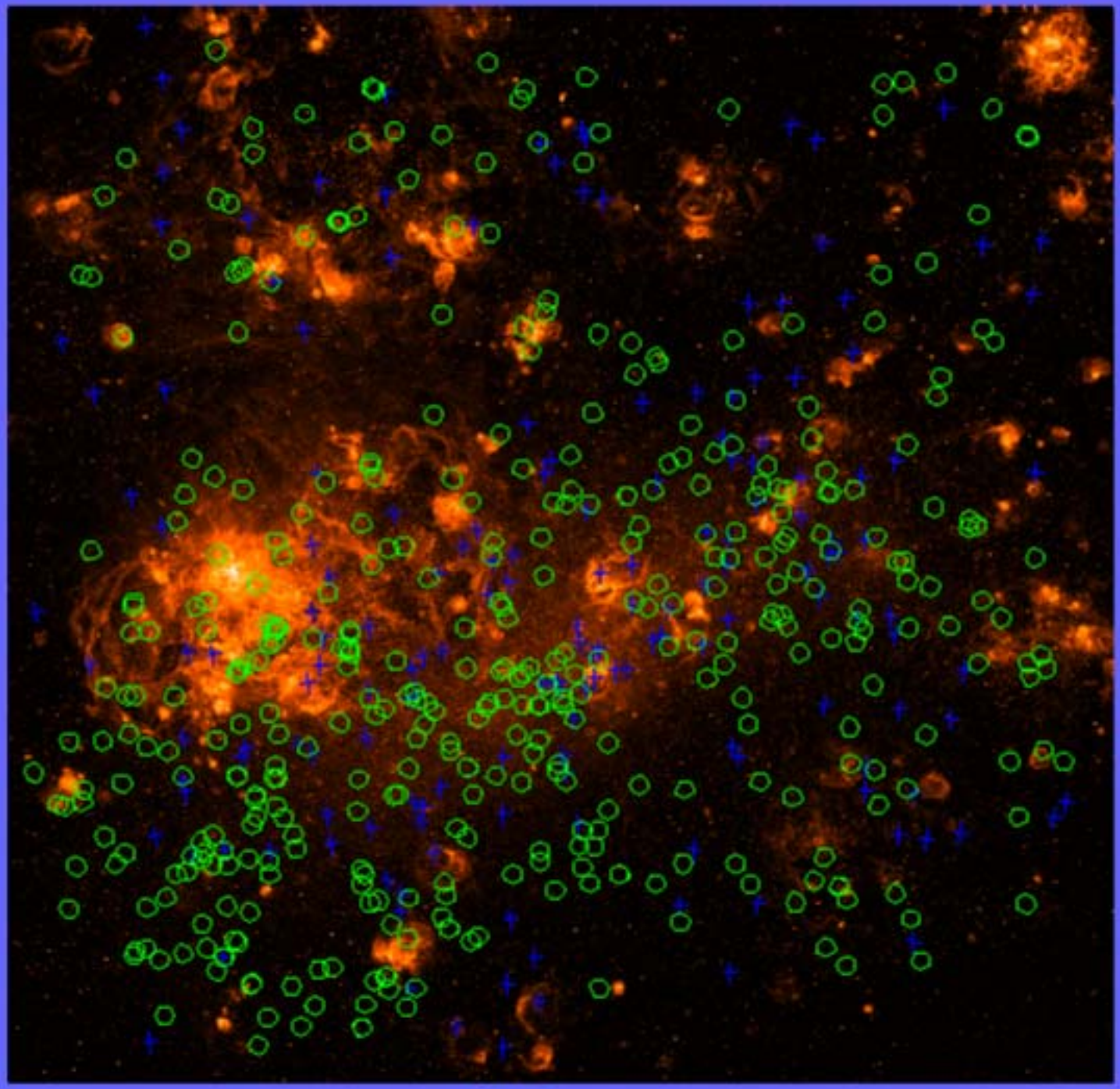

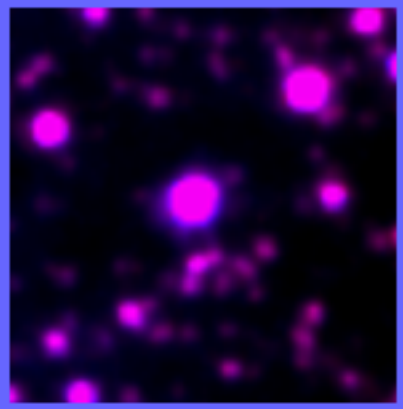

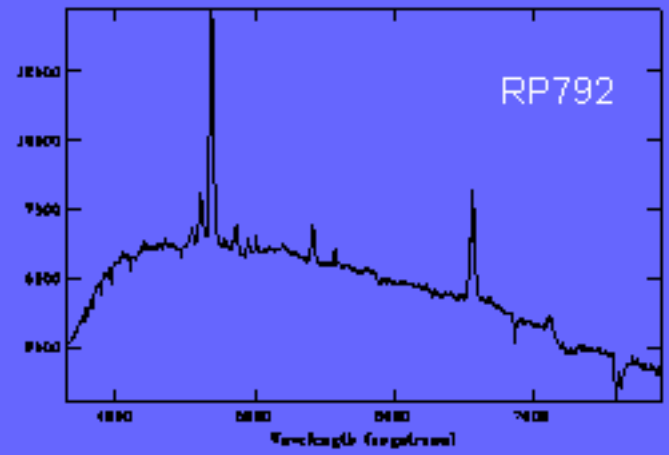

Previously known WR star

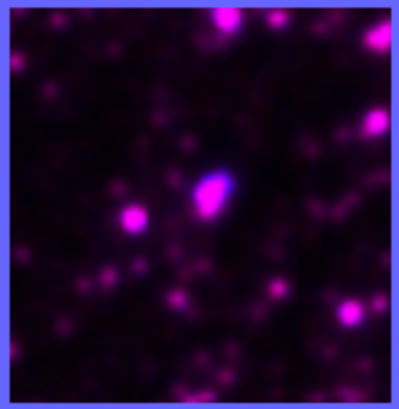

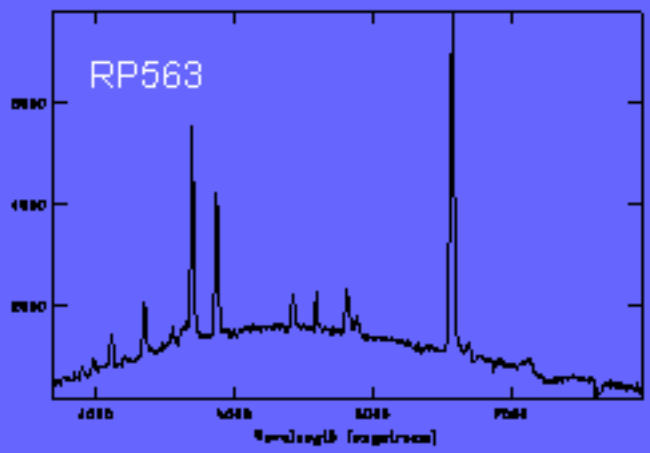

Newly discovered WR star

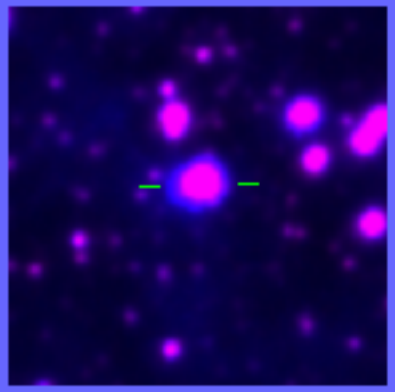

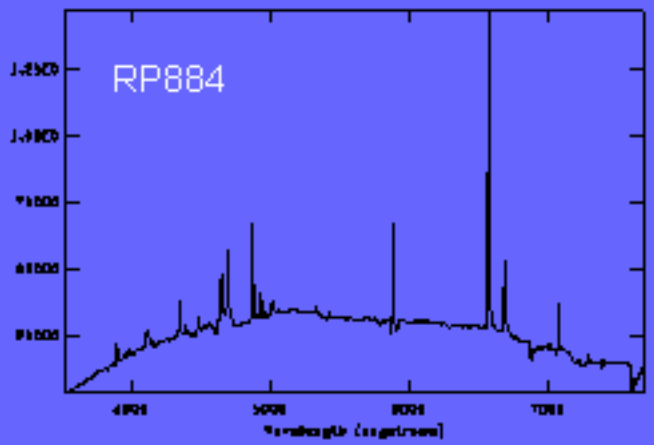

Newly discovered WR star

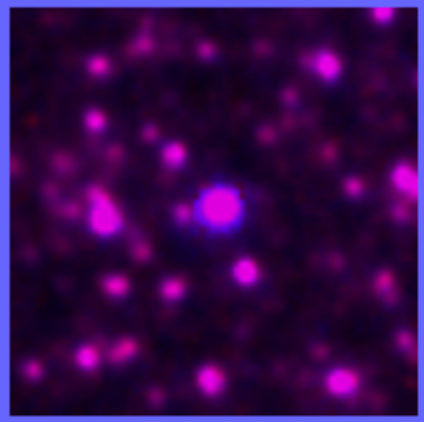

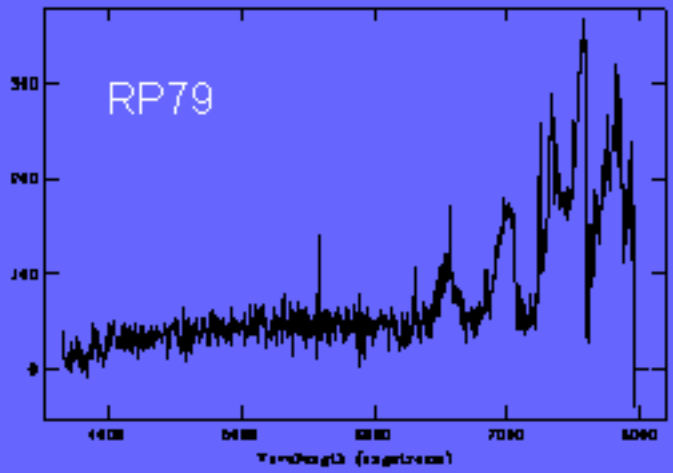

Previously known variable star

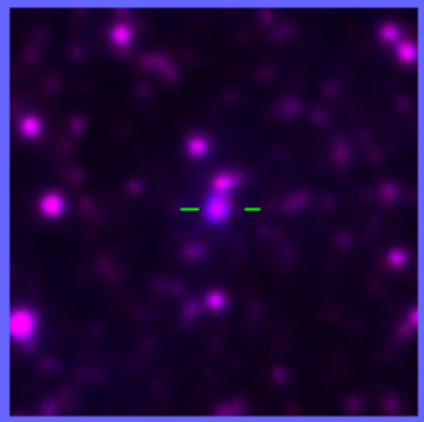

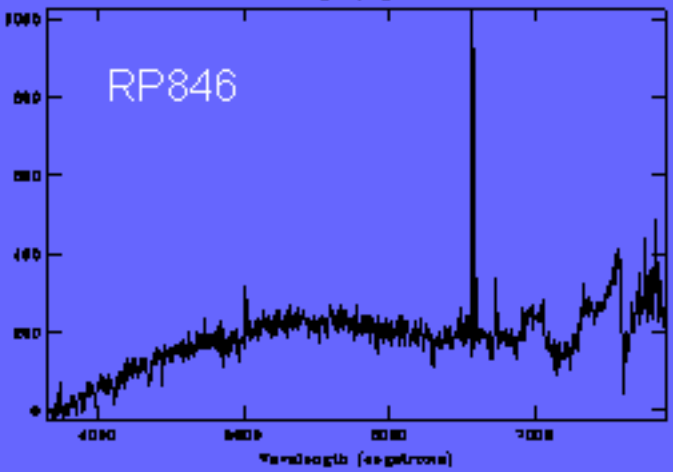

Newly discovered variable star

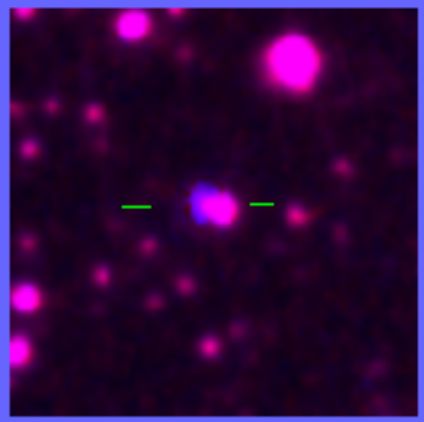

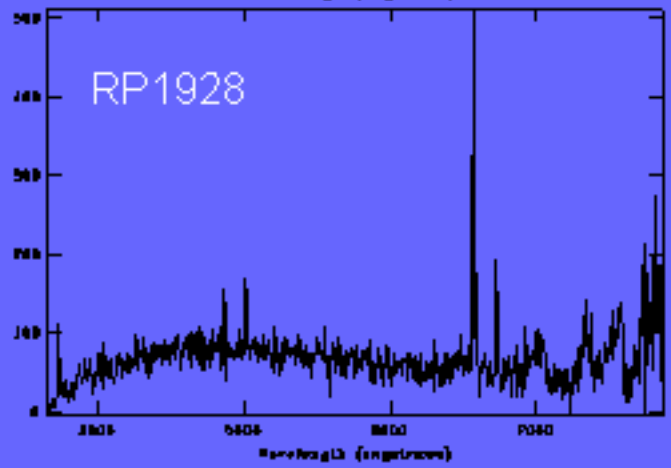

Newly discovered variable star

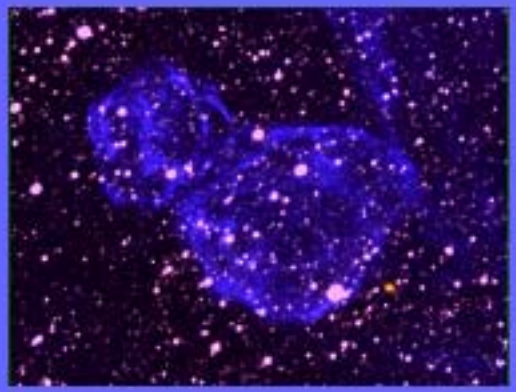

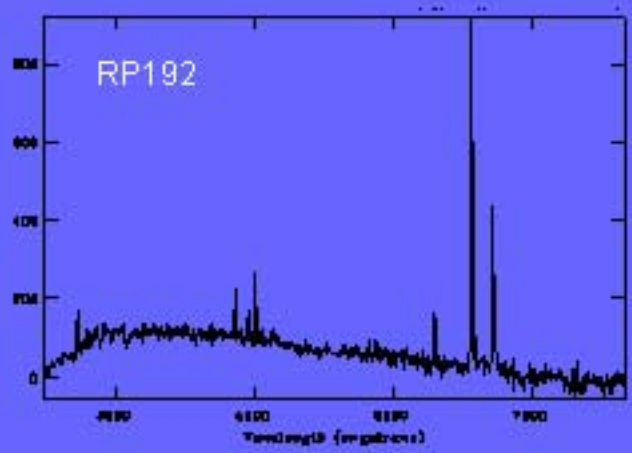

Previously known SNR

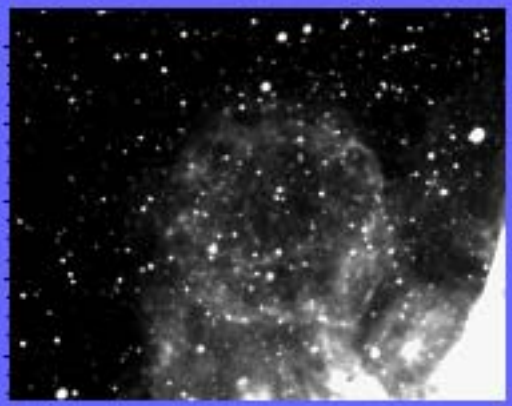

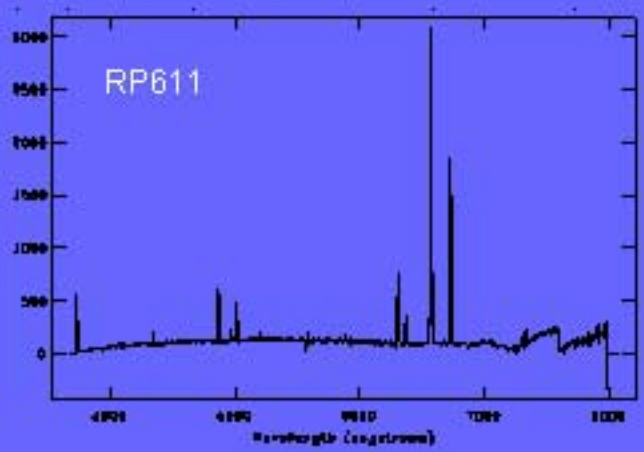

Newly discovered SNR

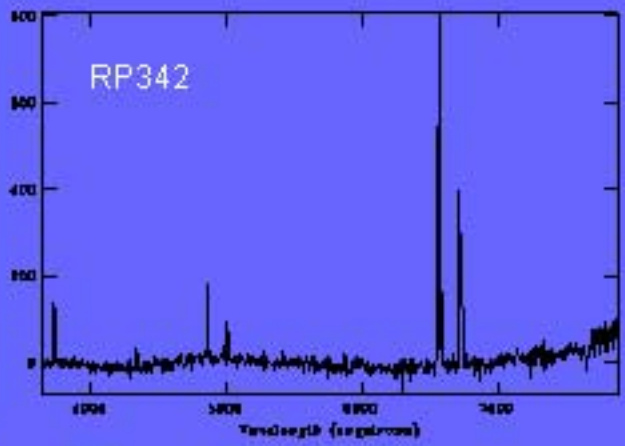

Newly discovered SNR

HST confirmation of RP PNe

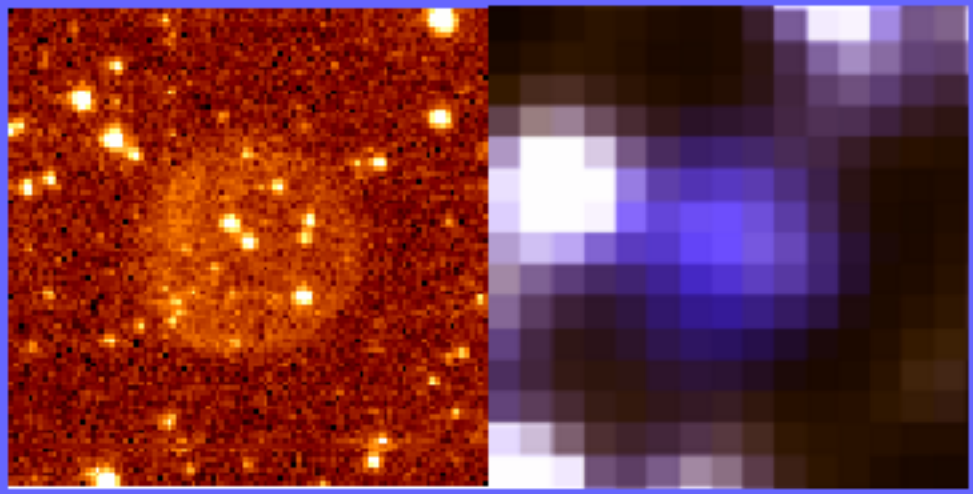

RP671

Left: HST image taken with WFPC2/F656N, Right: UKST discovery image

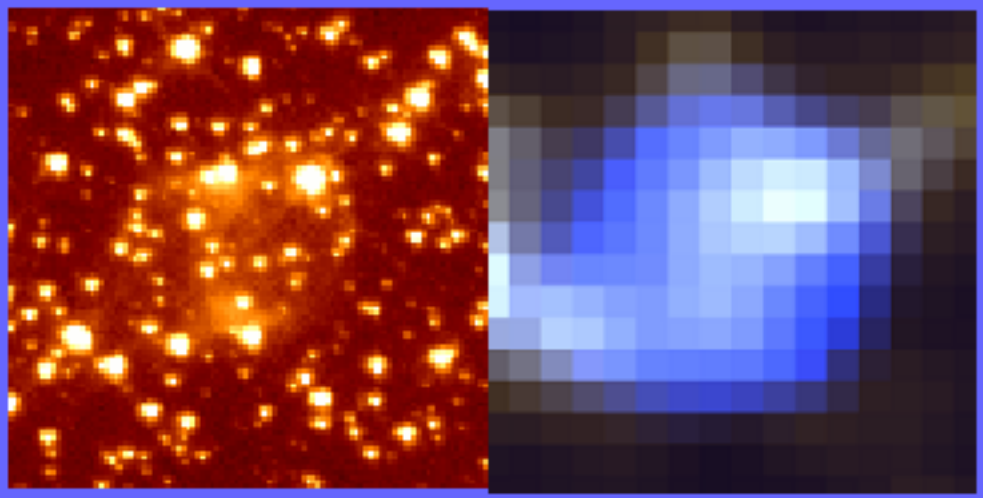

RP764

Left: HST image taken with WFPC2/F606W, Right: UKST discovery image

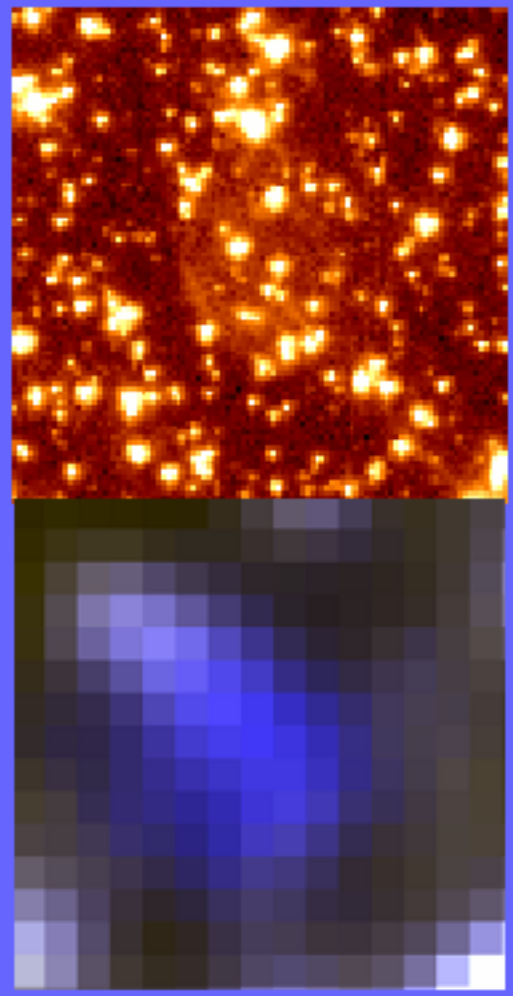

RP723

Above: HST image taken with WFPC2/F555W,
Below: UKST discovery image

Spectral diagnostics

Extinction

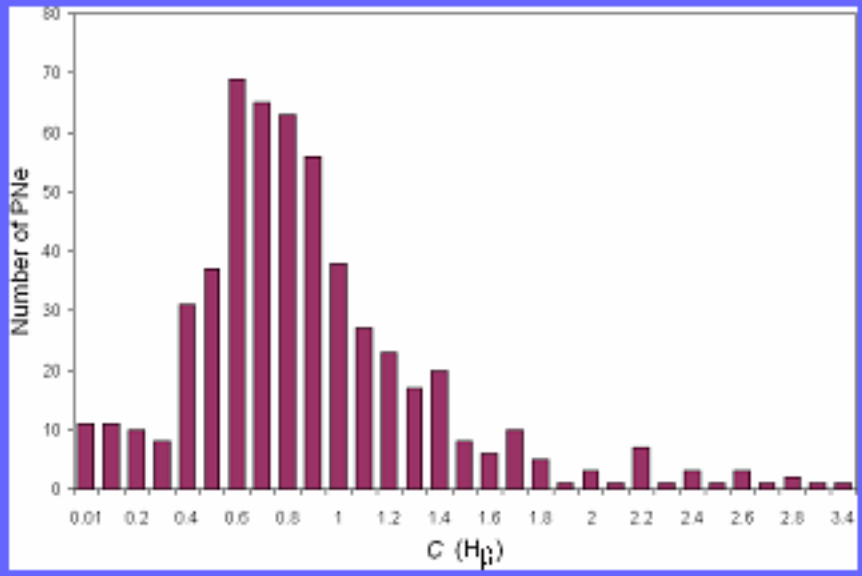

A peak at 0.6 shows the low overall extinction of most LMC PNe. Most of the bright PNe occupy the range 0.1-0.6.

$$c(\mathrm{H}\beta) = 2.875\ log(\mathrm{H}\alpha/\mathrm{H}\beta)/2.85$$

This estimation is based on the relationship between observed and intrinsic intensities:

$$\frac{I_{obs}(\mathrm{H}\alpha)}{I_{obs}(\mathrm{H}\beta)} = \frac{I_{int}(\mathrm{H}\alpha)}{I_{int}(\mathrm{H}\beta)}\ 10^{-c(\mathrm{H}\beta)[f(\mathrm{H}\alpha)-f(\mathrm{H}\beta)]}$$

All other lines were corrected for reddening using:

$$\frac{I_{cor}(\lambda)}{I_{cor}(\mathrm{H}\beta)} = \frac{I_{obs}(\lambda)}{I_{obs}(\mathrm{H}\beta)}\ 10^{cf(\lambda)}$$

Spectral diagnostics

Electron temperatures

[NII]

$$\frac{I(\lambda 6548 + \lambda 5683)}{I\,\lambda 5755} = 1.625 \times 10^{-2} \frac{1 + 1.94 * 10^{5}\, T_e^{1/2} / n_e}{1.03 + 3.20 * 10^{2}\, T_e^{1/2} / n_e}\, e^{25{,}000 / T_e}$$

[OIII]

$$\frac{I(\lambda 4959 + \lambda 5007)}{I(\lambda 4363)} = \frac{7.15 * 10^{14300 / T_e}}{1 + 0.028\,(10^{-4}\, n_e / T_e^{1/2})}$$

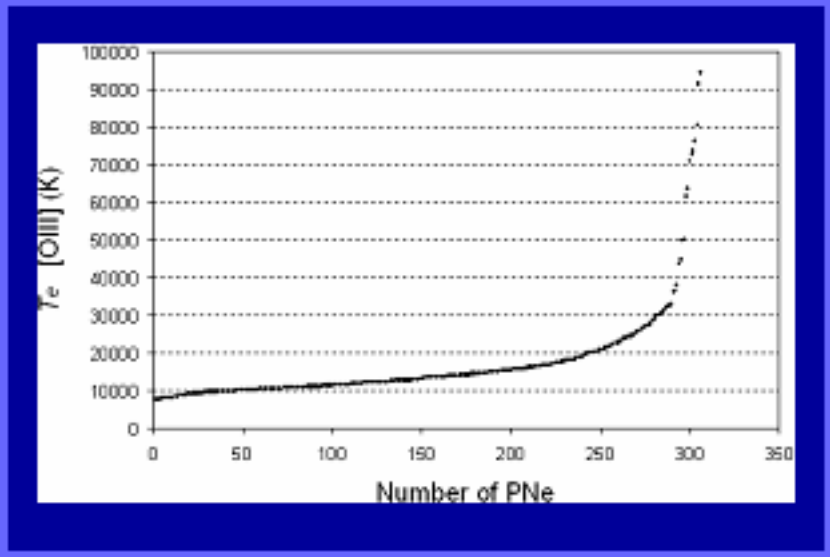

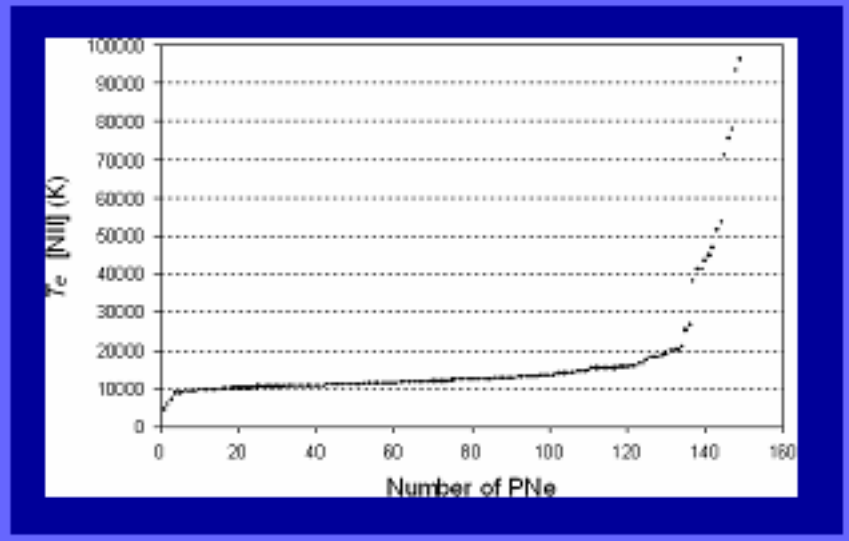

Spectral diagnostics

Electron densities

$$\frac{I\lambda 6717}{I\lambda 6731} = 1.5\,\frac{1 + 0.35x}{1 + 0.96x} \qquad \text{where } x = 10^{-2}\,\frac{n_e}{T_e^{1/2}}$$

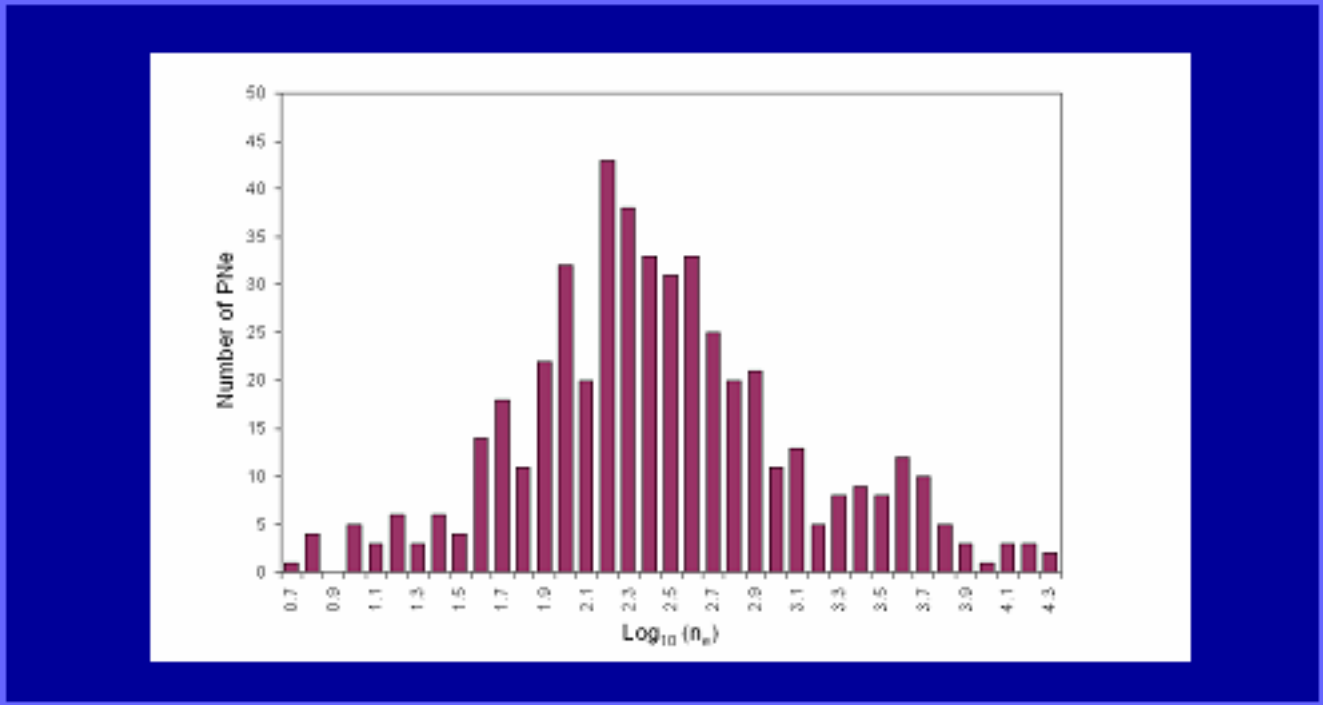

Densities for 483 LMC PNe

Spectral diagnostics

Nebula Masses

$$M_{neb} = 4\,\pi\,D^2\,F_{H\beta}\,(1+4y)\,m_H\,/\,(\alpha_{eff}\,h\nu\,n_e)$$

Where D is the distance to the LMC (50kpc), y = N(He)/N(H) = 0.11 (average value), α is the effective recombination coefficient of hydrogen for the emission of Hβ photons of energy $h\nu$ ($\alpha_{eff}h\nu$ = 1.24 x 10^{-25} ergs cm^{-3} s^{-1})

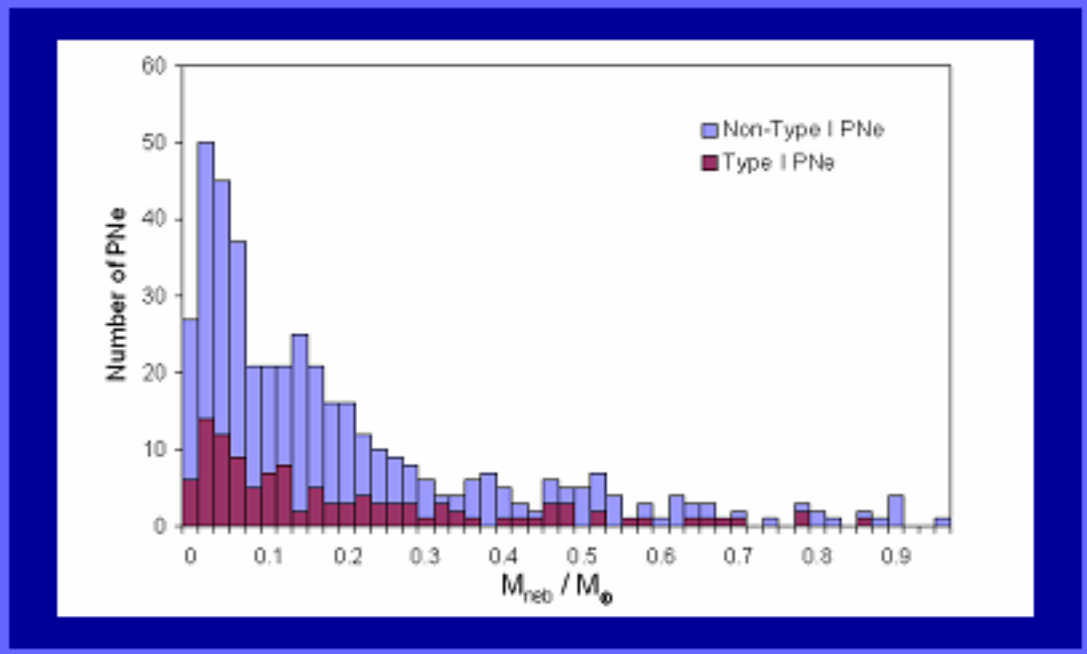

Spectral diagnostics

Density-to-mass relation

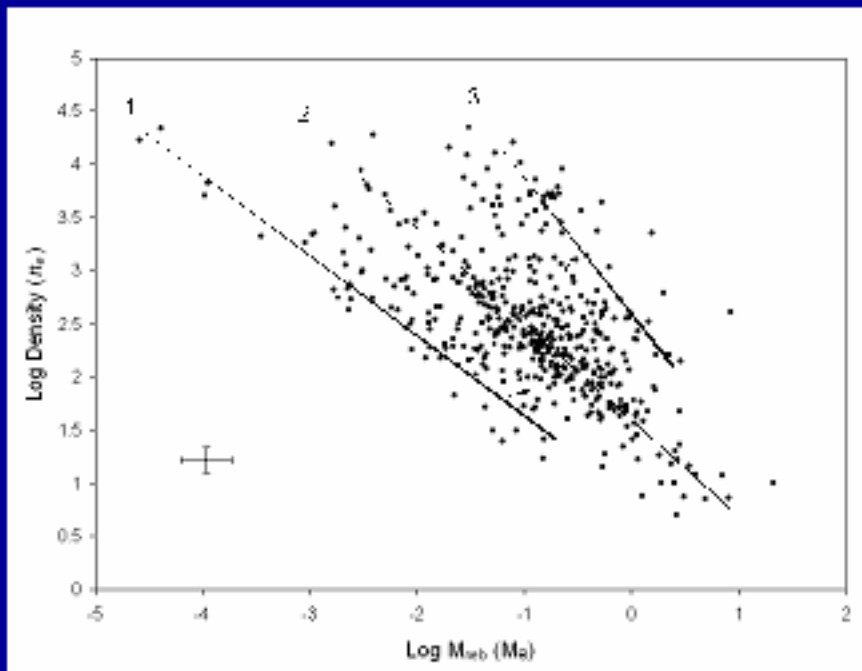

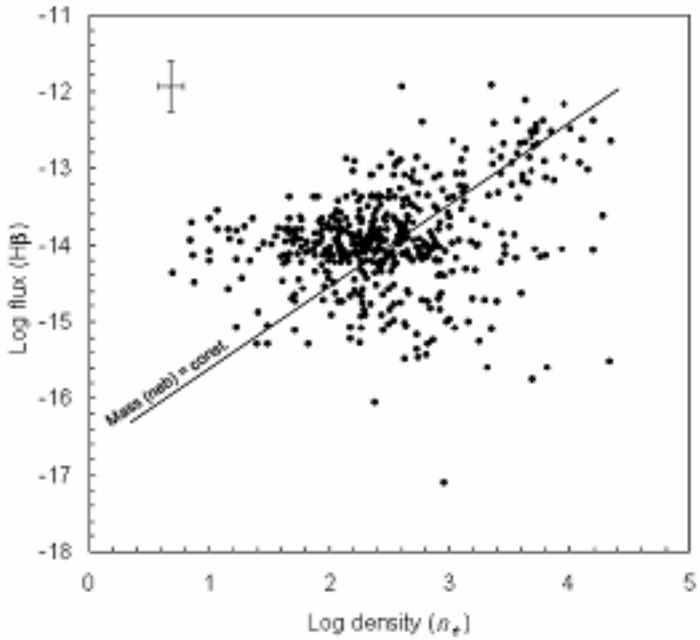

Spectral diagnostics

Excitation classes

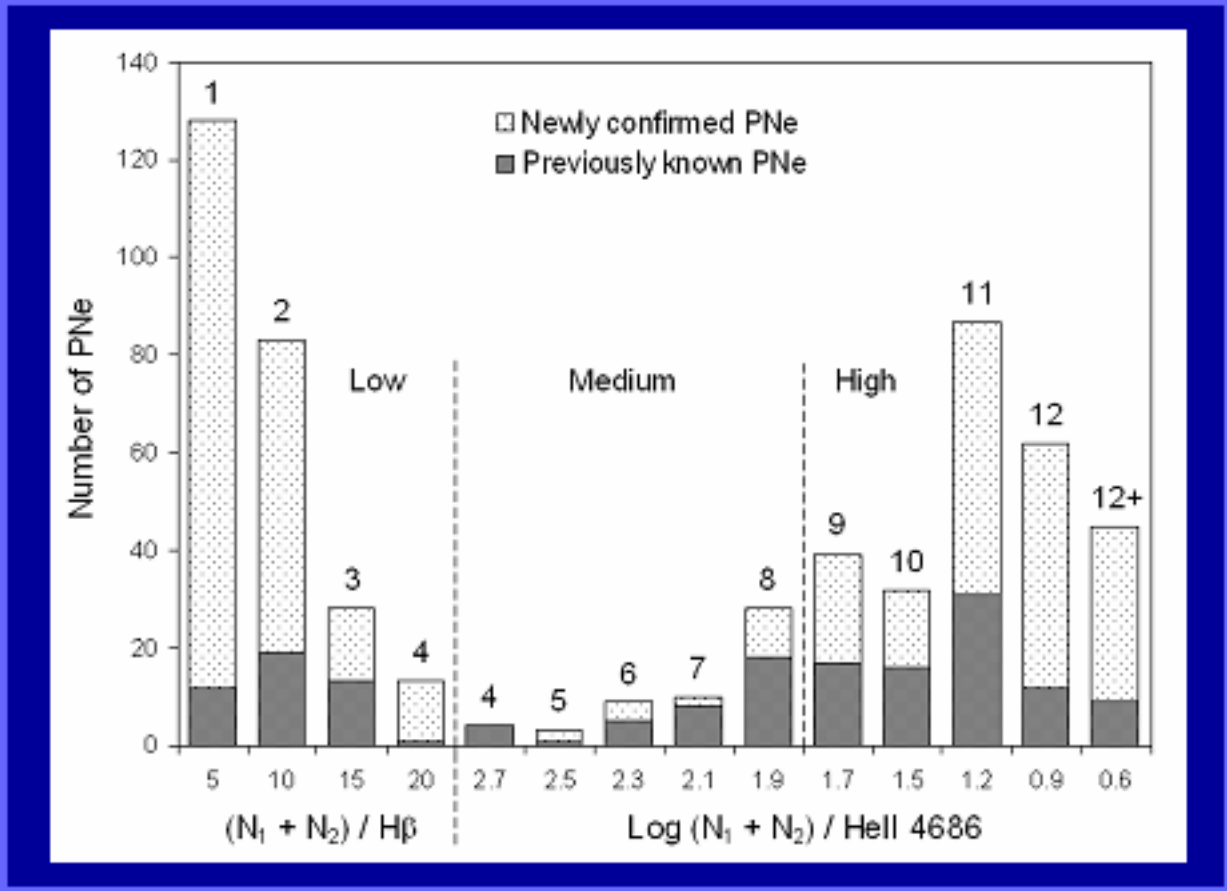

The classification is dependent upon [OIII] λ4959 + 5005 / H*β* for low excitation PNe and log [OIII] λ4959 + 5005 / He II λ4686 for medium and high excitation PNe.

Spectral diagnostics

The relationship of excitation class to mass, density and luminosity

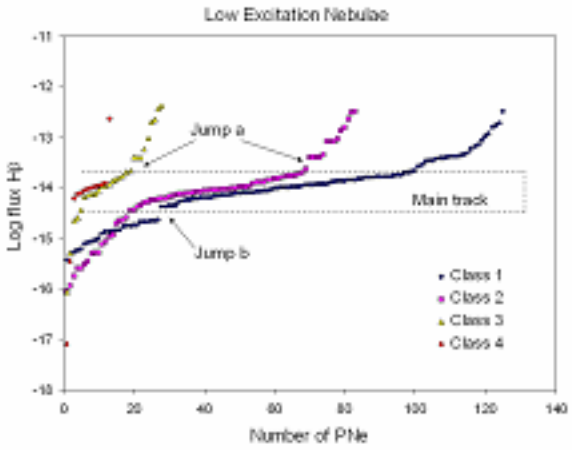

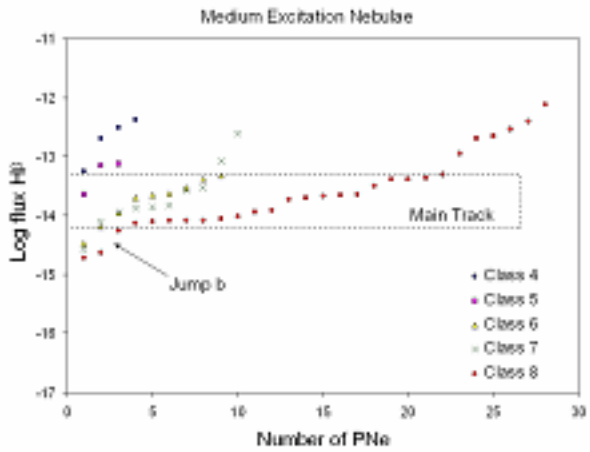

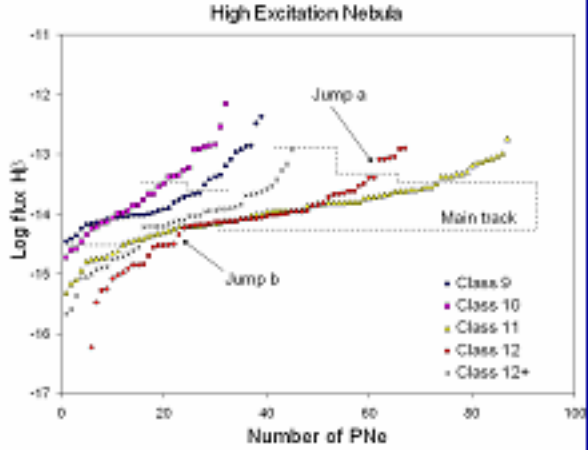

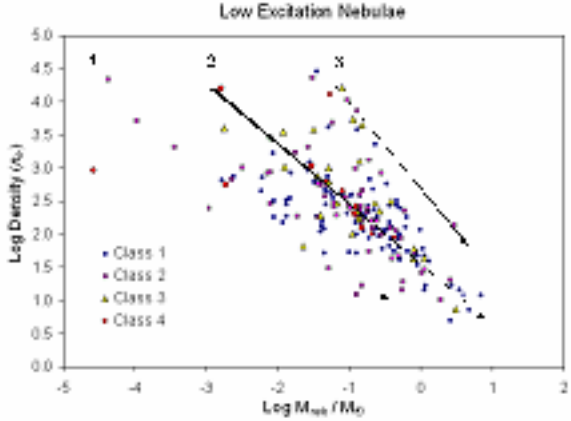

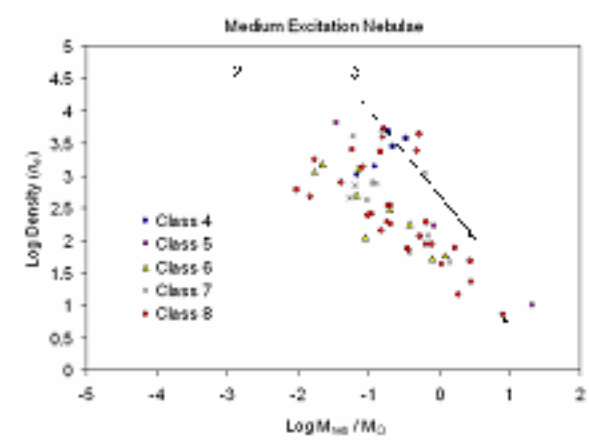

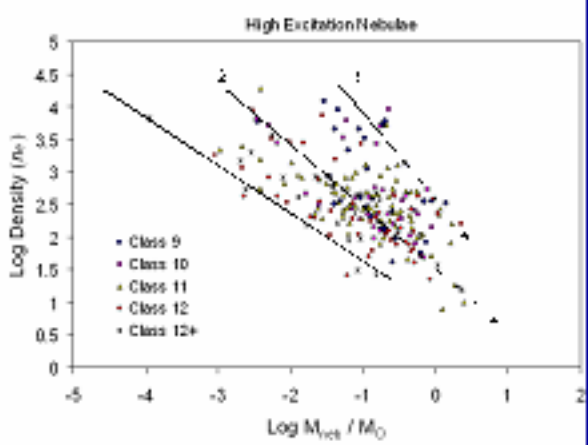

Spectral diagnostics

Dynamical age

$T_{dyn} = 890\ (M_{neb}\, V_{exp})^{0.6}\ yr$

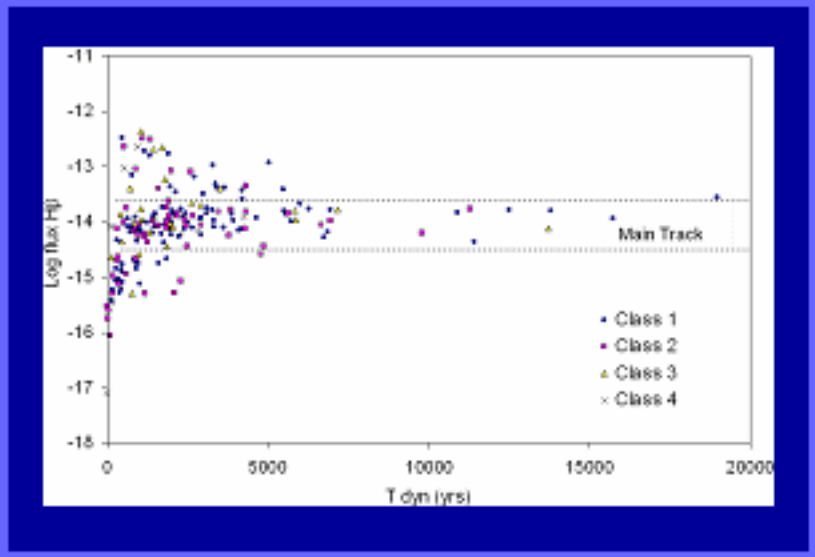

Low excitation

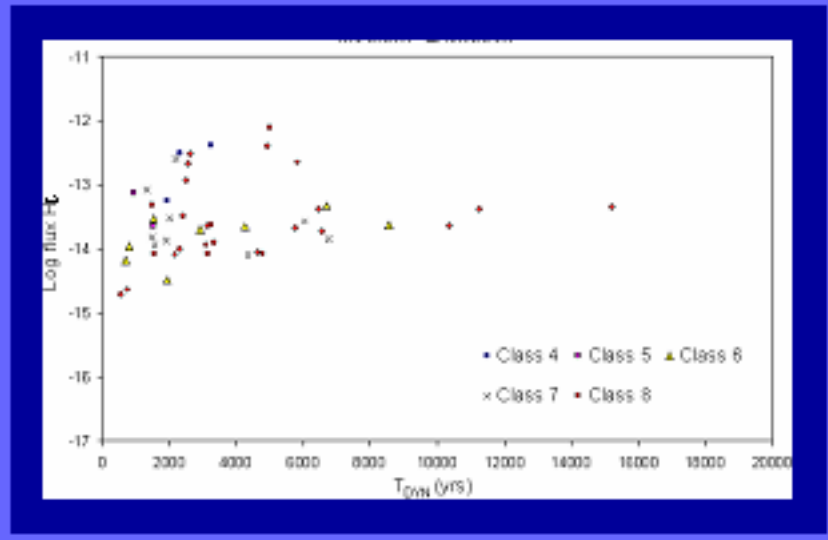

Medium excitation

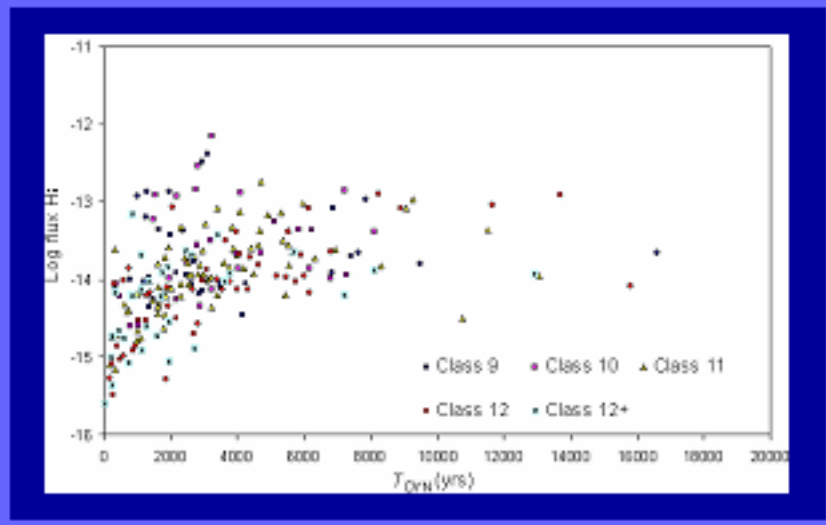

High excitation

Spectral diagnostics

Expansion velocity versus nebula mass

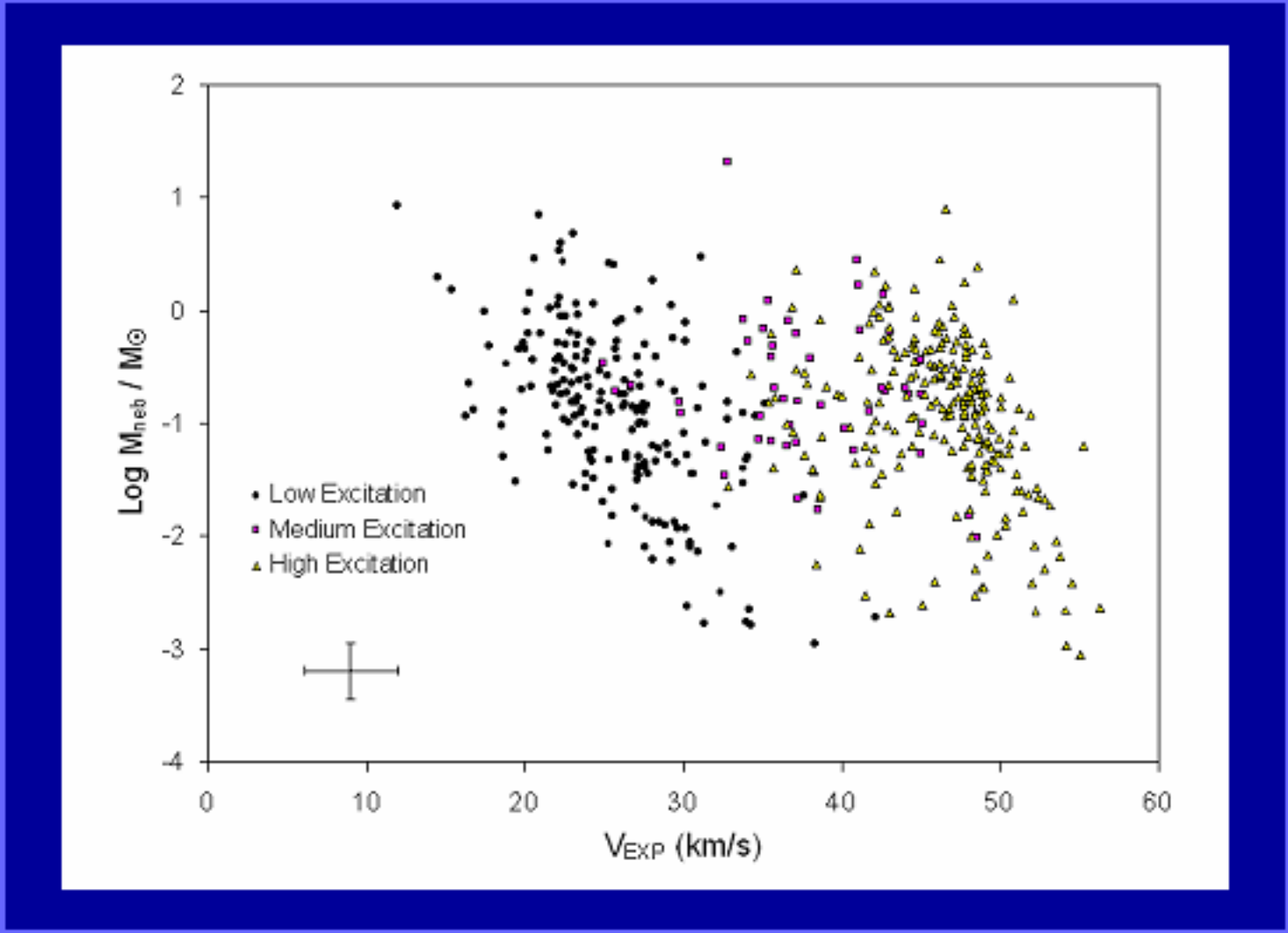

Planetary Nebula Luminosity function

Now extends over 10mag range
- faint end shape elucidated

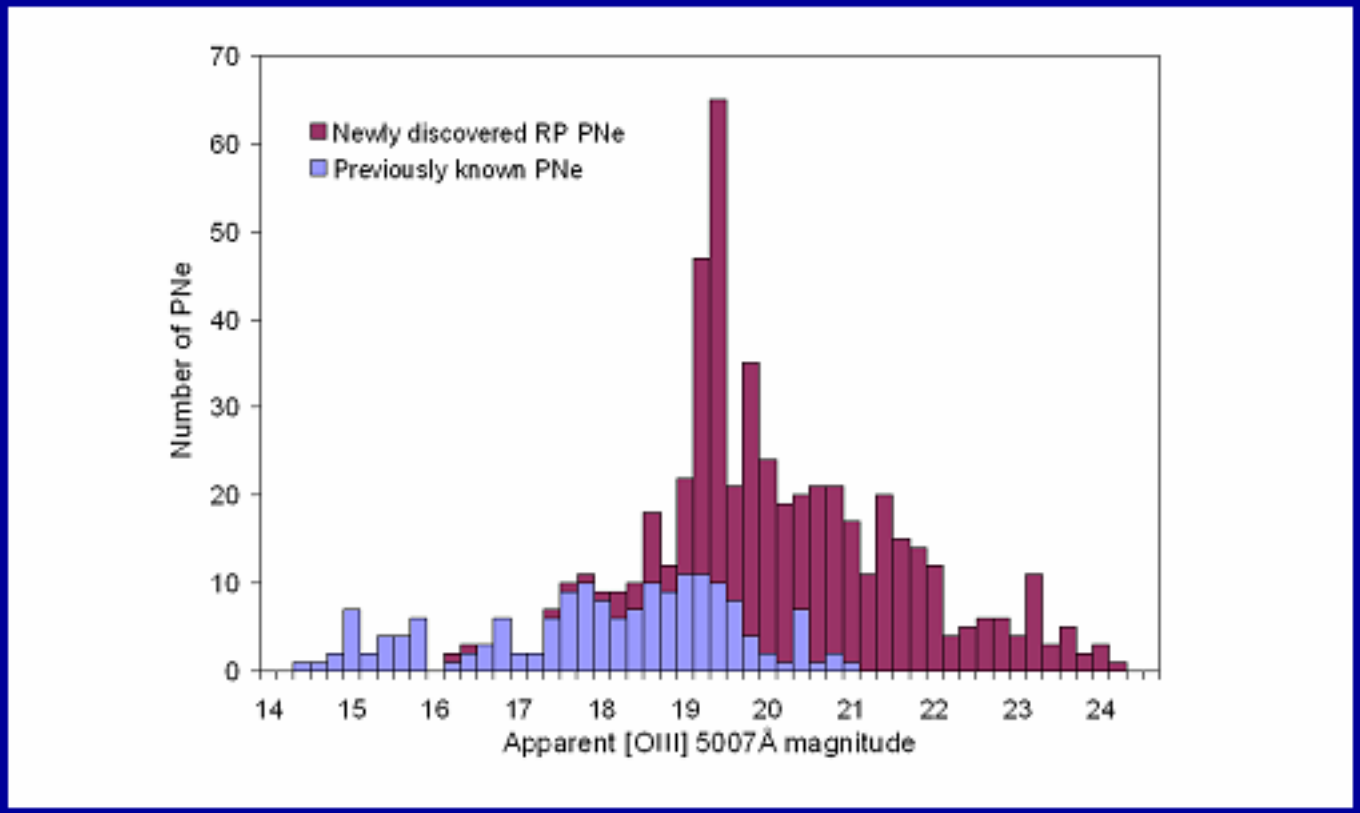

Planetary Nebula Luminosity function

PNLF as a distance indicator

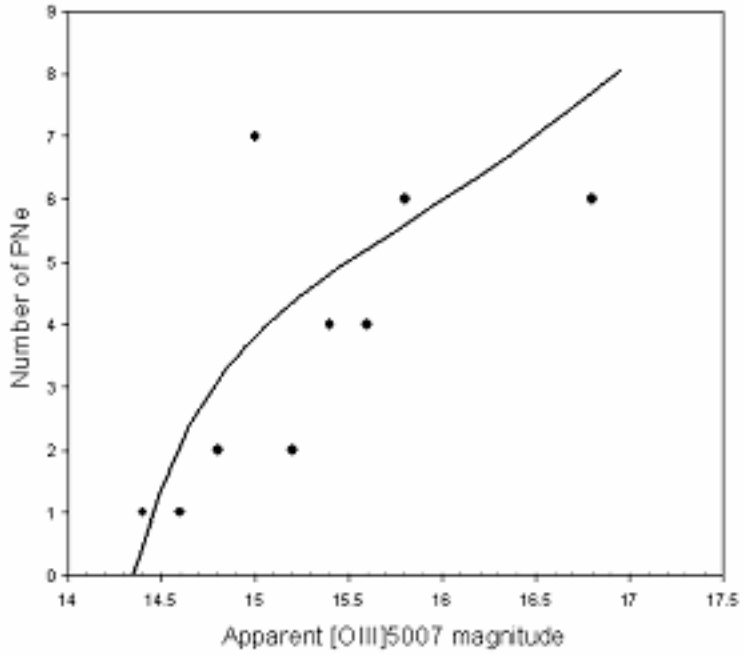

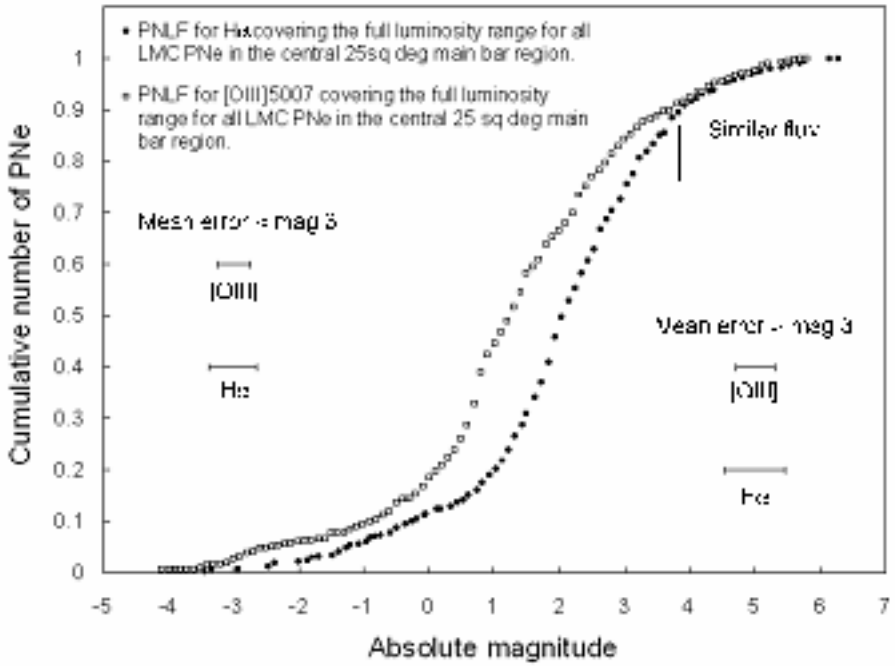

$$N(M) = e^{0.307M}\{1 - e^{3(M^* - M)}\}$$

Abundances

Method

An empirical method of abundance determination, similar to that of Aller (1984) has been used. It is the system which applies ionisation correction factors (ICFs) based on grids of photoionisation models of nebulae as used by Kingsburgh & Barlow (1994). The measured intensity ratios of the lines emitted by the ions provide the abundance ratio. For example, the ratio O^{++}/H^{+} is derived by:

$$O++ / H = \frac{[OIII]\lambda 5007 / H\beta}{^{j}[OIII]_{(Te,ne)} / ^{j} H\beta_{(Te)}}$$

Where $^{j}[OIII]_{(Te,ne)}$ is the emission coefficient of the [OIII]5007Å line which depends on T_e and n_e and $^{j} H\beta_{(Te)}$ is the emission coefficient of Hβ, which depends on T_e. The total oxygen abundance relative to hydrogen is then found by adding all of its ions so that:

$$O/H = O^{+} / H^{+} + O^{++} / H^{+} * ICF\ O$$

Aller L.H., 1984, Physics of Thermal Gaseous Nebulae, vol.112, Astrophysics and Space Science Library, D. Reidel Dordrecht, Holland.
Kingsburgh R.L., Barlow M.J., 1994, MNRAS 271, 257

Abundances

Type I PNe

He / H > 0.10 and $N^+/O^+ > 0.25$

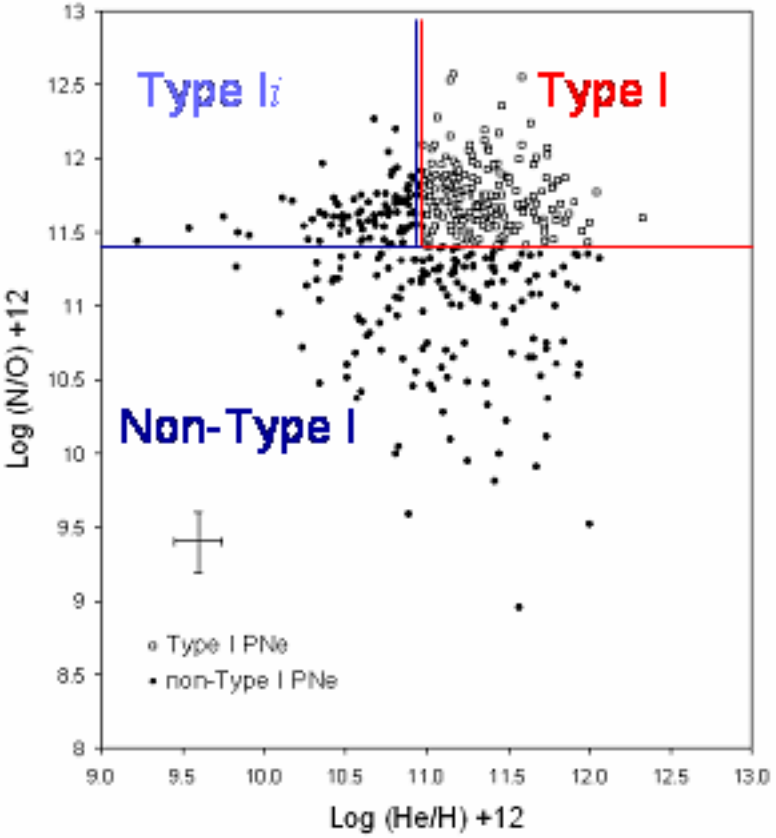

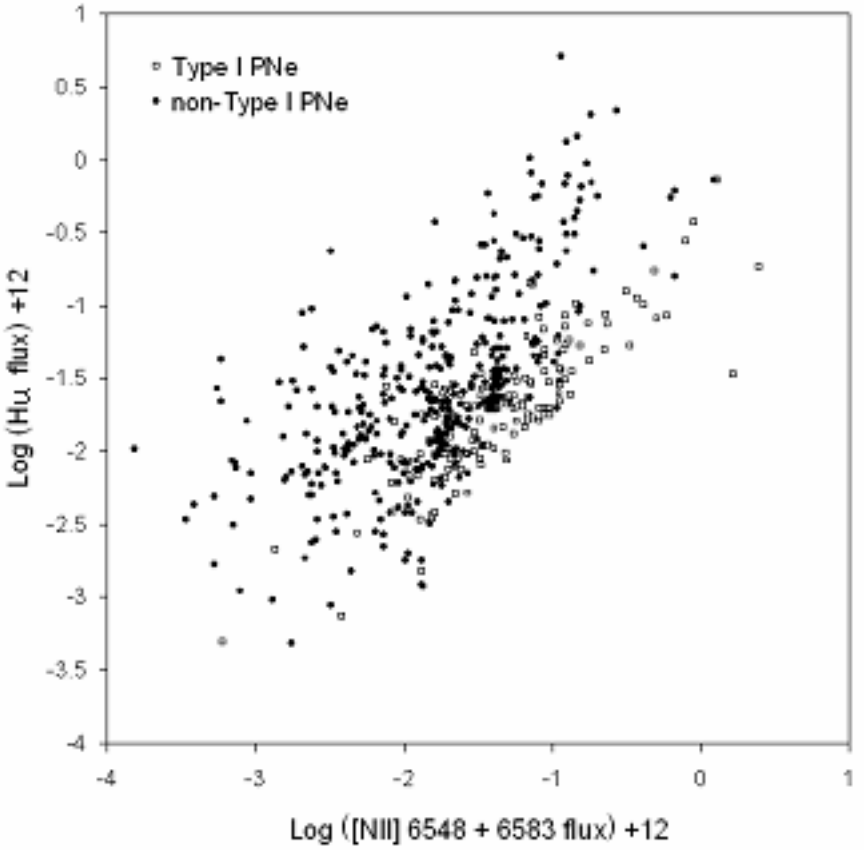

Abundances

N/O plot for 37 LMC PNe from Dopita & Meatheringham 1991, ApJ. 377, 480

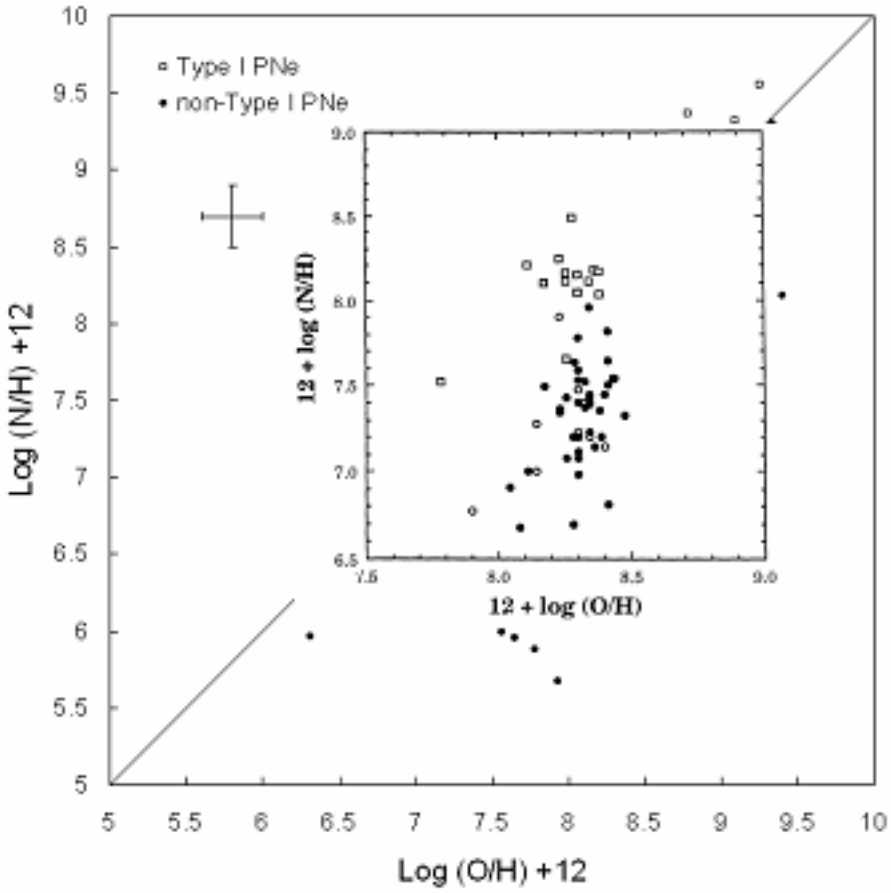

N/O plot for 360 LMC PNe from Reid, Ph.D. thesis, 2007

Radial Velocities

The need for an accurate and comprehensive LMC PN velocity study

Survey	Telescope	Res. or Disp.	λ for V_R	V_R disp (km/s)	N_{PNe}	$V_{grad\ max}$ degrees
Feast 1986	74" SAAO	49Å/mm	Hγ	22±3	25	171
Webster 1969	74" MSO	140,50Å/mm	3 R, 6 B	24±5	24	171
Smith & Weedman 1972	36" CTIO		[O III] 5007	14.7	27	171
Meatheringham et al. 1988	1-m, 2.3-m,	11.75 km/s	[O III] 5007	20	94	-
"	3.9-m AAT					
Borcson & Liebert 1989	2.5-m LCO	3.5Å/pixel	Hβ, [O III] 5007	-	24	-
Vassiliadis et al 1992	2.3-m SSO	11.5 km/s	[O III] 5007	-	16	-
Morgan & Parker 1998	1.2-m UKST	1.34Å/pixel	cross cor	-	96	-
"			4550-5500Å			
This work	3.9-m AAT	1.1Å/pixel	6200-7300Å	20.6±8	587	122

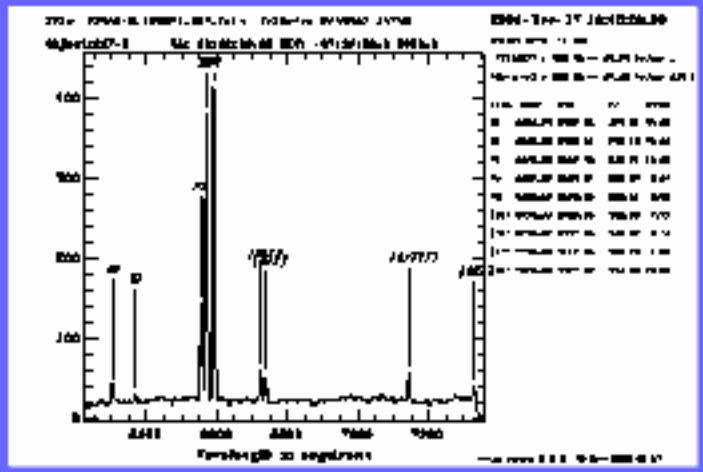

Emission line

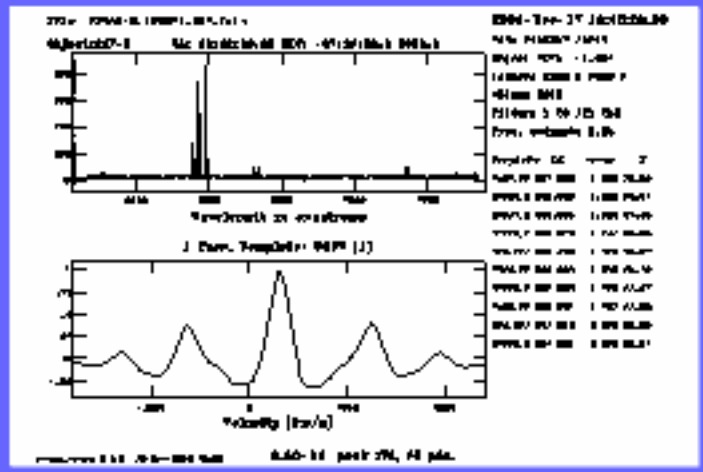

Cross-correlation

PN kinematics within the LMC

A PN radial velocity map of the central 25 deg^2 of the LMC

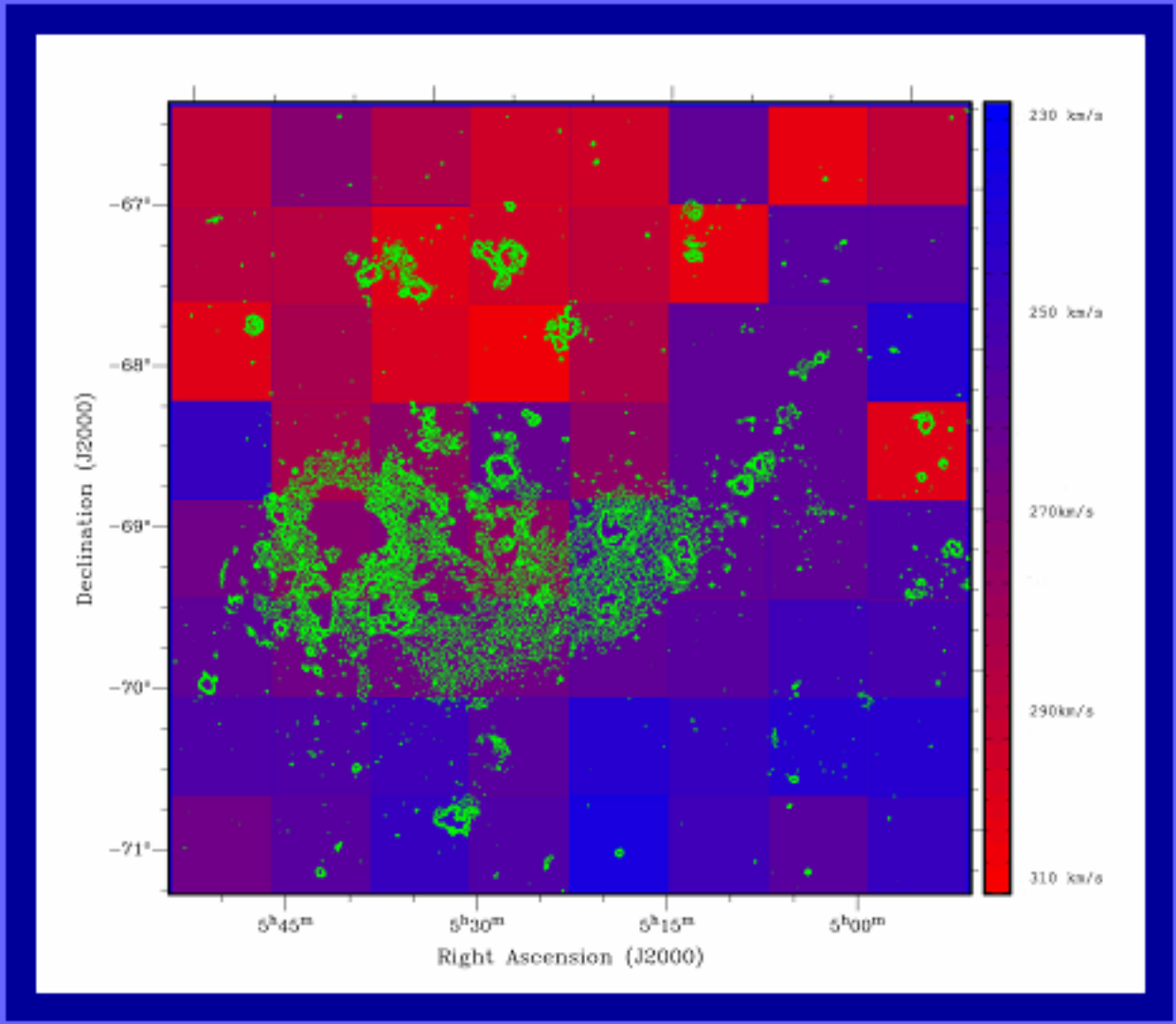

PN kinematics within the LMC

Comparison of PN and HI radial velocities

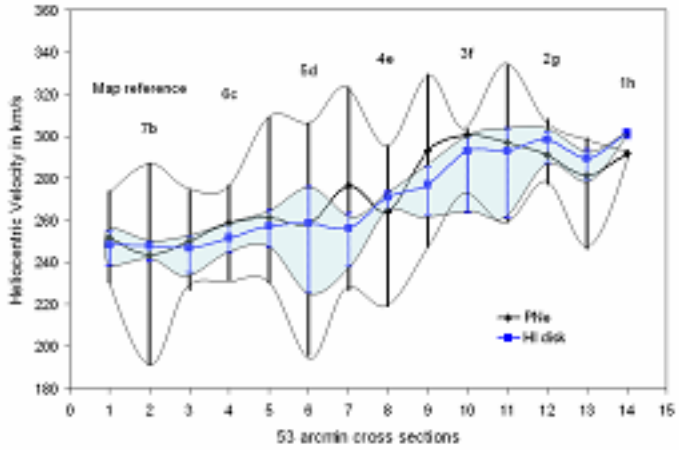

PN kinematics within the LMC

Rotation curves for PNe and HI

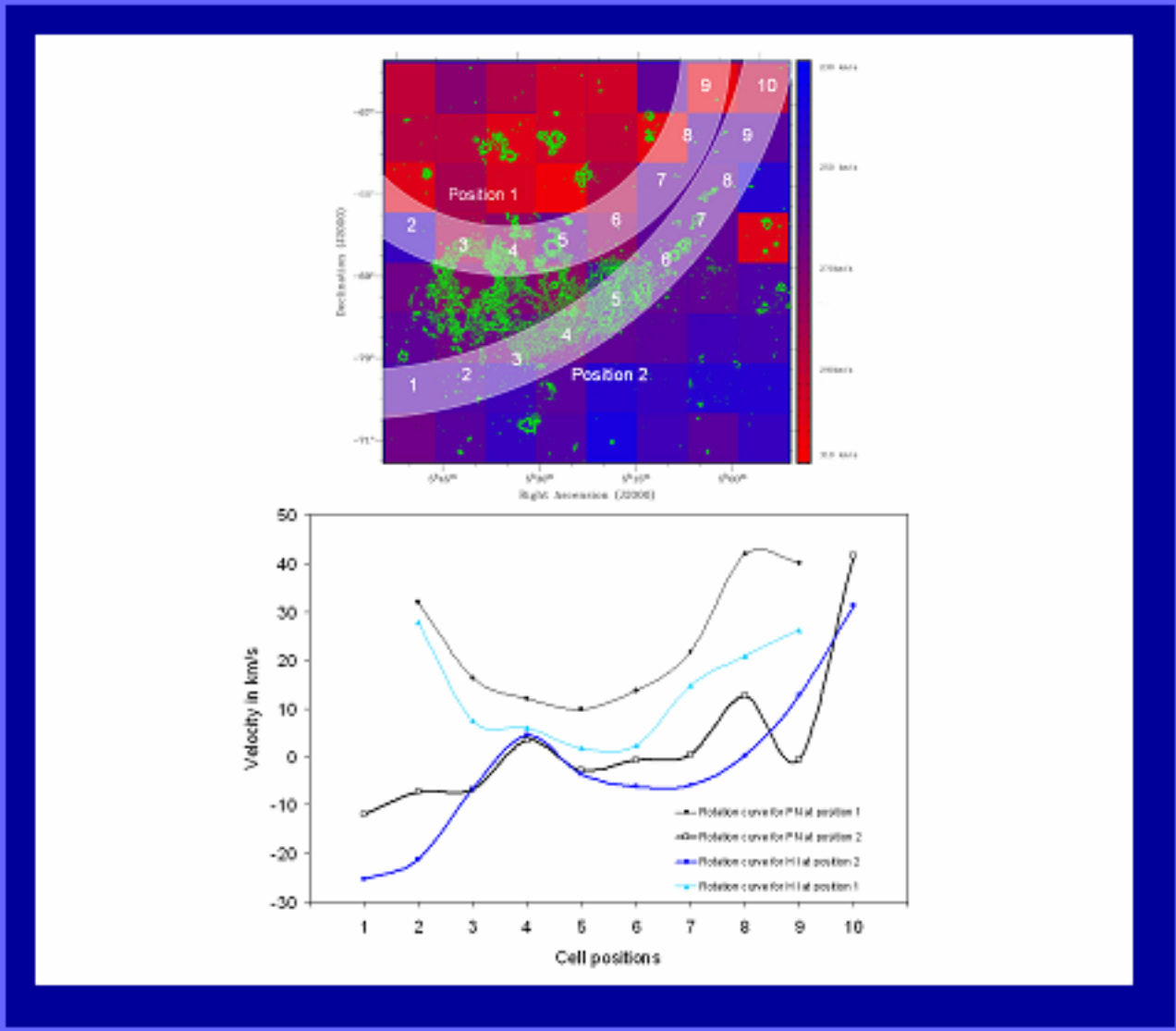

Summary

Parameter	Previous results	New results
Number of PNe in the central 25 deg^2 region of the LMC	164	623
Estimated number of PNe in the entire LMC	~1,000	956±141
PN magnitude range ([O III] 5007Å)	6	10
Range in cHβ for LMC PNe	0.00 - 1.3	0.01 - 3.4
Peak in cHβ distribution	0.3	0.6
Range in [O III] electron temperatures t_e	> 10,600 K	7,728 - 95,307 K 80% under 20,000K
Range in [N II] electron temperatures t_e	> 7,800 K	4,646 - 96,799 K 90% under 20,000K
Range in electron densities n_e	log (2 - 4.56) g cm^{-3}	log (1 - 4.8) g cm^{-3}
Peak in n_e distribution	log 3.6 g cm^{-3}	log 2.2 g cm^{-3}
Range in Mass$_{neb}$	0.02 - 0.94 M$_\odot$	0.01 - 0.97 M$_\odot$
Peak in Mass$_{neb}$ distribution	0.09	0.2 M$_\odot$
Number of low excitation PNe Number of medium excitation PNe Number of high excitation PNe	45 (27%) 36 (23%) 81 (50%)	247 (43%) 63 (11%) 261 (46%)
Range in derived V$_{exp}$	5.1 - 82 km s^{-1}	9.7 - 82 km s^{-1}
Mean Oxygen abundance (log +12) Mean Nitrogen abundance (log +12) Mean neon abundance (log +12) Mean sulphur abundance (log +12) Mean argon abundance (log +12)	8.1 - 8.49* 7.23 - 8.26* 7.39 - 7.80* 6.67 - 6.92* 5.88 - 6.00*	8.10 ±0.49 7.67 ±0.60 7.32 ±0.87 6.29 ±0.66 5.83 ±0.67
No. of Type I PNe in survey region	67	183
ISM nitrogen enhancement in the LMC due to PNe	6.8 × 10^{-7} M$_\odot$ yr^{-1}	2.02 × 10^{-6} M$_\odot$ yr^{-1}
Bright turnoff magnitude (M*) Distance to LMC using PNLF	-4.1 48.7 kpc	-4.1 48.7 kpc
Peak of PNLF distribution	unknown	0.6 Mag (absolute)
No. LMC PNe Vel$_{rad}$ measurements	97	587
Mean PN vertical velocity dispersion Mean HI vertical velocity dispersion	19.1 km s^{-1} 5.4 km s^{-1}	40.1 km s^{-1} 18 km s^{-1}
PN centroid (J2000) Vel$_{GSR}$ at PN centroid	05^{h}23^{m}23^s -68°58^m unknown	05^{h}19^{m}12^s -69°26^{m}17^s 70.7 km s^{-1}